Web crippling of lean duplex stainless steel tubular sections under concentrated end bearing loads

Yancheng Cai *, Ben Young

Department of Civil Engineering, The University of Hong Kong, Pokfulam Road, Hong Kong

Abstract

A series of tests was conducted to investigate the web crippling behaviour of cold-formed lean duplex stainless steel (LDSS) tubular sections. The LDSS had two grades, including EN 1.4062 and EN 1.4162. The tests were performed under three different conditions of concentrated end bearing loads, namely, the loading conditions of End-One-Flange (EOF), the End-Two-Flange (ETF) and end loading (EL). The loading conditions of EOF and ETF are specified in the American and Australian/New Zealand cold-formed stainless steel design specifications, while the loading condition of EL simulated the floor joist members positioned on a solid foundation under concentrated end bearing load. The test specimens were mainly failed by web crippling. The test strengths were compared with the predicted strengths that calculated by the stainless steel design specifications, including the American Society of Civil Engineers (ASCE) Specification, Australian/New Zealand Standard (AS/NZS) and European Code (EC). In addition, the web crippling strengths predicted by the North American Specification (NAS) for cold-formed carbon steel structures and using the design equations proposed in the literature for cold-formed duplex stainless steel tubular sections were also compared with the test strengths. It was found that the predicted strengths calculated by the ASCE, AS/NZS and EC specifications are conservative and reliable for LDSS sections under the three different concentrated end bearing loads. The predictions by NAS and proposed equations in the literature are generally less conservative compared with those by ASCE, AS/NZS and EC. However, the predictions by NAS are found to be unconservative and not reliable for the loading condition of ETF.

Keywords: Cold-formed, concentrated end bearing loads, experimental investigation, lean duplex stainless steel, web crippling.

* Corresponding author. Tel.: +852-2859-2665.
E-mail address: yccai@hku.hk (Y. Cai).

1. Introduction

Lean duplex stainless steel (LDSS), including grades EN 1.4062 and EN 1.4162, is a relatively new material, and has recently gained significant attention in construction industry due to its exceptional mechanical properties, good corrosion resistance and lower cost compare to its counterpart of duplex stainless steel type. The material cost of stainless steel is sensitive to the alloy content, in particular the level of nickel [1]. LDSS only contains approximately 1.5% of nickel (Ni) compared to 5-8% in duplex stainless steel and 8-10% in austenitic stainless steel. Hence, the cost of LDSS is reduced significantly compared with duplex stainless steel grades, due to the lower nickel content. In the past few years, significant progress has been made on the behaviour of LDSS structural members, including material properties [2], beams [1, 3-4], columns [1, 5-7], beam-columns [8-9], plate girders [10-11], as well as single shear [12-14] and double shear bolted connections [12, 15].

Webs of steel tubular sections may cripple under high concentrated bearing loads. This is because it is not easy to stiffen the webs of steel tubular sections. Therefore, web crippling strength should be checked carefully if the steel tubular sections were under concentrated bearing loads. Research on web crippling failure of cold-formed stainless steel lipped channel sections were conducted by Korvink and van den Berg [16] and Korvink et al. [17]. The tubular sections were then tested by Talja and Salmi [18] and Gardner et al. [19], in which the sections were cold-formed from austenitic stainless steel. Zhou and Young [20-22] conducted a series of tests on web crippling of cold-formed stainless steel tubular sections, including austenitic stainless steel under loading conditions of End-Two-Flange (ETF) and Interior-Two-Flange (ITF) [20], duplex stainless steel under loading conditions of End-One-Flange (EOF), Interior-One-Flange (IOF), ETF and ITF [21] as well as austenitic and duplex stainless steel under end loading (EL) and interior loading (IL) [22]. Recently, the tubular sections of cold-formed ferritic stainless steel that subjected to web crippling were investigated by Bock et al. [23] and Li and Young [24]. However, there is presently no experimental investigation on the web crippling behaviour of cold-formed LDSS tubular sections under concentrated bearing loads.

The web crippling design rules are specified in the current international stainless steel specifications, i.e., American Society of Civil Engineers (ASCE) Specification [25], Australian/ New Zealand Standard (AS/NZS) [26] and European Code (EC3-1.4) [27]. However, these design rules for stainless steel members are mainly adopted from those of carbon steel members [20]. In addition, the cold-formed LDSS is not included in the current

ASCE [25] and AS/NZS [26] stainless steel design specifications, while it was recently introduced in the EC3-1.4 code [27]. It should be noted that EC3-1.4 [27] does not have specific design rules for web crippling of stainless steel sections and may refer to those specified in the EC3-1.3 [28]. In this study, a series of tests was conducted to investigate the web crippling behaviour of LDSS tubular sections under concentrated end bearing loads.

Totally 50 tests on cold-formed LDSS tubular members were conducted. The LDSS members including EN 1.4062 and EN 1.4162, had square and rectangular hollow sections. The sections were subjected to three different concentrated end bearing loads, namely, loading conditions of the End-One-Flange (EOF), ETF and EL. The loading conditions of EOF and ETF are specified in the ASCE [25] and AS/NZS [26] specifications, while the loading condition of EL simulated the floor joist members under concentrated bearing load. The strengths obtained from the tests were compared with the predicted strengths calculated using the ASCE [25], AS/NZS [26] and EC3-1.4 [27] stainless steel specifications. In addition, the web crippling strengths predicted by the North American Specification (NAS) [29] for cold-formed carbon steel structures and using the design equations proposed by Zhou and Young [30] for cold-formed duplex stainless steel tubular sections were also compared with the test strengths. The reliability of the aforementioned web crippling design provisions was assessed by reliability analysis.

2. Experimental investigation

2.1. Test specimens and bearing plates

Totally 50 cold-formed LDSS tubular members of square and rectangular hollow sections were tested. The LDSS had two grades of EN 1.4062 and EN 1.4162. The measurements on the dimensions of the cross-sections were recorded. These include the height of web (H), width of flange (B), the section thickness (t) and the section inner radius (r_i). The values of measured web heights were in the range of 19.9 to 152.0 mm, flange widths in the range of 20.1 to 151.9 mm, thicknesses in the range of 1.49 to 3.10 mm, and inner radii in the range of 0.8 to 6.5 mm. In addition, the web slenderness ratios (h/t) ranged from 9.8 to 43.5. The test specimens with the measured dimensions are shown in Tables 1-3, with the nomenclature of the section defined in Fig. 1. The length (L) of each specimen was designed by referring to the NAS [29] and the measured values are also shown in Tables 1-3. For the loading condition of EOF, the clear distance of 1.5H was designed between the bearing edges of adjacent opposite concentrated loads or reactions; while for the loading conditions of ETF and EL, the similar

1.5*H* clear distance was designed but from the specimen end to the bearing plate edge, as illustrated in Fig. 2(a)-(c).

Steel bearing plates were used to transfer the applied loading or reaction into the specimens. A total of six steel bearing plates with 50 mm thickness having different dimensions were produced. The steel bearing plates were long and wide enough to cover the full section flange width, except for the rounded corners. Generally, different bearing lengths were used for each section. Hence, the effect of different bearing lengths was also investigated. In this experimental investigation, all flanges of the LDSS tubular sections were not fastened to the steel bearing plates.

2.2. Specimen labelling

The LDSS specimens were labelled in order to identify the loading conditions (EOF, ETF and EL), nominal section dimensions as well as the bearing length, as shown in Tables 1-3. For examples, the specimens of "EOF120×60×3.0N30", "ETF120×60×3.0N30" and "EL120×60×3.0N60-r" represent the following. The two or three letters in the front of the label mean that the LDSS tubular section was tested under the loading condition of End-One-Flange (EOF), End-Two-Flange (ETF) or End loading (EL). The next segment shows the nominal dimension of the specimen section ($H \times B \times t$), namely, 120×60×3.0 means H = 120 mm, B = 60 mm and t = 3.0 mm. The last segment N30 or N60 means that the specimen was loaded subjected to a bearing length of 30 or 60 mm. The repeated test was indicated by the last letter "r" in the label.

2.3. Material properties

Tensile coupon specimens were designed based on the ASTM Standard [31], with 12.5 mm width and 50 mm gauge length. They were cut from the tubular sections in the longitudinal direction in the centre face of the web or flange at 90-degree angle from the weld. The coupon specimens were tested in an MTS 810 testing machine by displacement control. The longitudinal strain of the coupons was measured by strain gauges at both sides of the gauge length and a calibrated MTS extensometer with 50 mm gauge length. They were recorded together with the applied load at regular intervals by a data acquisition system. The tests were conducted in accordance with the procedure suggested by Huang and Young [32]. The material properties of cold-formed LDSS obtained from the tensile coupons are detailed in Table 4.

The compressive coupon tests were conducted by extracting the compressive coupons from the untested LDSS tubular sections. Generally, they were extracted in transverse direction from the webs in which the corresponding specimen sections were tested. If there is welding in the section webs, then the compressive coupons were cut from the face opposite to the weld, including sections ($H\times B\times t$) of 50×20×1.5, 60×40×2.0, 60×120×3.0 and 80×150×3.0 in this study. The nominal length and width of the compressive coupons in this study were 48 mm and 25 mm, respectively. However, for the sections of 50×20×1.5, 60×40×2.0 and 60×120×3.0, the nominal length and width of the coupons were 26 mm and 13 mm, respectively, due to the limited heights of the webs. The tests were conducted in accordance with the procedure detailed in Li and Young [24]. The material properties of cold-formed LDSS obtained by compressive coupon tests are detailed in Table 5.

2.4. Test rig and operation

Tests of the cold-formed LDSS tubular hollow sections were conducted by concentrated end bearing loads, namely, the loading conditions of EOF, ETF and EL. The loading conditions of EOF and ETF are specified in the ASCE [25] and AS/NZS [26] stainless steel specifications, while the loading condition of EL simulated the floor joist members on a solid foundation under concentrated bearing load. The loading condition of EL is not specified in the ASCE [25] and AS/NZS [26] stainless steel specifications.

For the loading condition of EOF, two steel bearing plates having the same width and thickness were positioned at the specimen ends. The steel bearing plates were connected onto the load transfer plates. Two identical rollers were used to support the load transfer plates. Hence, the symmetrical supporting condition of the test specimen at the two ends could be achieved. A steel plate having twice the width of the steel bearing plate was set at mid-span of the test specimen. The steel plate was fixed to a half round, and it transferred the applied load to the top flange of the specimen. Steel stiffening plates were used to prevent web failure of the specimen at mid-span. They were set at both sides of the specimen. The width of the stiffening plates and the load transfer plate at mid-span are identical. At each end of the test specimen, two calibrated linear variable displacement transducers (LVDTs) were used to measure the vertical web deformation of the specimen. The measurements covered the deformations between the steel bearing plates and the top flanges of specimen near the corners. In addition, another two LVDTs had flat plastic plates at the ends were positioned at both sides of the specimen webs. It should be noted that the plastic plates were rigidly

connected to the end of the LVDTs. The plastic plates covered the specimen webs in an area that was able to capture the maximum web deformations in lateral direction. At the failure specimen end, the average readings of the two LVDTs were used for the vertical and lateral web deformations, respectively. The test setup of Specimen EOF150×80×3.0N90 is illustrated in Fig. 3(a), with the corresponding schematic view as shown in Fig. 2(a).

For the loading condition of ETF, the end of the test specimen was loaded by using two identical steel bearing plates. The steel bearing plates were positioned at the top and bottom flanges of the specimen. The steel bearing plates were fixed to the two half rounds. The applied load was transferred to the specimen flanges by the steel bearing plates through the half rounds. Four calibrated LVDTs were positioned to measure the vertical web deformations of the test specimen. The lateral web deformations of the test specimen were measured in a similar way as those for the loading condition of EOF. The test setup of Specimen ETF80×150×3.0N150 undergoing ETF loading condition is illustrated in Fig. 3(b), with the corresponding schematic view as shown in Fig. 2(b). While for the loading condition of EL, only one steel bearing plate was used. The steel bearing plate was fixed to a half round and positioned at the top flange of the test specimen at the end in order to transfer the applied concentrated load. The arrangements of the LVDTs for the measurements of vertical web deformations and lateral web deformations are identical to those for the measurements in the ETF loading condition. The test setup and schematic view for Specimen EL100×100×3.0N30 under EL loading condition are shown in Fig. 3(c) and Fig. 2(c), respectively, where the specimen was positioned on a fixed flat solid base plate.

The compressive force was applied to the test specimens by a load testing machine. The tests were carried out by displacement control. The loading rate of 0.3 mm/min was used for all the tests. The applied load from the machine and the readings from the LVDTs were recorded by a data acquisition system regularly during the tests.

2.5. Test results

Tables 1-3 reported the test strengths per web (P_{test}) for the cold-formed LDSS specimens undergoing the loading conditions of EOF, ETF and EL, respectively. All the LDSS tubular sections under concentrated end bearing loads were failed by web crippling, except for three specimens, EOF50×20×1.5N30, EOF60×120×3.0N90 and EOF100×100×3.0N90, that failed near the mid-span. Repeated tests were conducted on specimens ETF40×60×2.0N60,

ETF60×40×2.0N30, ETF100×100×3.0N90, EL100×100×3.0N90, EL120×60×3.0N60 and EL150×80×3.0N90. The differences between the first and repeated test strength were 1.2%, 5.3%, 2.6%, 0.8%, 5.4% and 2.2%, respectively. Overall, the test results were reliable as the differences are relatively small. Figs. 4(a)-(b) exemplifies the load versus the web deformation curves for specimens EOF80×150×3.0N60, ETF60×40×2.0N30 and EL120×60×3.0N60. The vertical axis represents the applied load on the specimen, while the horizontal axis plots the measured vertical and lateral deformation of the specimen. The web crippling failure of specimens EOF150×80×3.0N90 ETF150×80×3.0N90 and EL150×80×3.0N90 that subjected to different loading conditions with the same bearing length is illustrated in Fig. 5(b)-(d).

3. Design rules

The design rules for sections failed by web crippling are provided in the current international stainless steel specifications [25-27]. The design rules specified in the AS/NZS Standard [26] and the ASCE Specification [25] are identical. Hence, the predicted web crippling strengths for these two specifications [25-26] are identical. The web crippling design rules in the EC3-1.4 [27] may refer to those specified in the EC3-1.3 Code [28]. In this study, the EC3-1.3 Code [28] was used to calculate the web crippling strengths of the cold-formed LDSS sections. In addition, the web crippling design rules specified in the NAS [29] were used, although the design specification is focused on cold-formed carbon steel structural members. This is because, as mentioned earlier in the "Introduction", the web crippling design provisions in the current stainless steel specifications are mainly adopted from those design provisions for carbon steel structures. The web crippling design rules proposed by Zhou and Young [30] for the cold-formed duplex stainless steel tubular sections were also assessed, as the grade of LDSS is close to that of the duplex stainless steel.

The ASCE Specification [25] provides web crippling design rules for sections with single webs under different support conditions of flanges for the degree of resistant against rotation of web. Hollow sections and lipped channel sections belong to sections with single web according to the ASCE Specification [25]. Hence, the design rules for sections with single webs were used in this study. The calculation of web crippling strengths for the sections under loading conditions of EOF and ETF was in accordance with Equations (1) and (2) of the ASCE Specification [25], respectively. Equations (1) and (2) are suitable for the sections with flanges stiffened or partially stiffened. Note that the current ASCE [25] or AS/NZS [26] specification does not specify design rules for EL loading condition. Hence, the web crippling

design under the EL loading condition used the same equation as those in the EOF and ETF loading conditions in this study.

EOF loading condition:

$$P_{ASCE} = t^2 C_3 C_4 C_\theta \left(2.28 - 0.042\frac{h}{t}\right)\left(1 + 0.01\frac{N}{t}\right) \quad (1)$$

ETF loading condition:

$$P_{ASCE} = t^2 C_3 C_4 C_\theta \left(1.68 - 0.004\frac{h}{t}\right)\left(1 + 0.01\frac{N}{t}\right) \quad (2)$$

where

$$C_3 = \begin{cases} (1.33 - 0.33k)k & if \ \ f_y \le 459\,\text{MPa} \\ 1.34 & if \ \ f_y > 459\,\text{MPa} \end{cases} \quad (3)$$

$$C_4 = \left(1.15 - 0.15\frac{r_i}{t}\right) \le 1.0 \qquad \text{but not less than 0.50} \quad (4)$$

$$C_\theta = 0.7 + 0.3\left(\frac{\theta}{90}\right)^2 \quad (5)$$

$$k = \frac{f_y}{228} \quad (6)$$

in which P_{ASCE} = the nominal web crippling strength per web predicted by ASCE [25], C_3, C_4, C_θ and k are coefficients; θ = the web inclination angle in degrees. Equations (1) and (2) are applicable for conditions of $45 \le \theta \le 90$, $N/t \le 210$ and $N/h \le 3.5$.

The EC3-1.4 [27] refers to EC3-1.3 [28] for the web crippling design rules of cold-formed stainless steel. The web crippling resistance in EC3-1.3 [28] is referred as the local transverse resistance. The design rules provided in Section 6.1.7.3 with the Equation 6.18 of the EC3-1.3 [28] are applicable to sections with two or more unstiffened webs. Tubular sections belong to sections with two or more unstiffened webs. Hence, the design rules in Section 6.1.7.3 with the Equation 6.18 of the EC3-1.3 [28] were adopted in this study. The web crippling resistance equation is shown in Equation (7).

$$P_{EC} = \alpha t^2 \sqrt{f_y E}\left(1 - 0.1\sqrt{\frac{r_i}{t}}\right)\left(0.5 + \sqrt{\frac{0.02 l_a}{t}}\right)\left[2.4 - \left(\frac{\theta}{90}\right)^2\right] \quad (7)$$

in which P_{EC} = the nominal web crippling strength per web predicted by EC [28], α is the web crippling coefficient, l_a is the effective bearing length, θ is the angle of the web relative to the flanges in degrees. Equation (7) is applicable for sections with $h/t \leq 200$, $r_i/t \leq 10$, $45 \leq \theta \leq 90$.

The values of α and l_a depend on the loading conditions as illustrated in Fig. 6.9 of EC3-1.3 [28] and shape of the section, i.e. sheeting profiles, liner trays and hat sections. The EOF, ETF and EL loading conditions in this study belongs to Category 1 according to the Fig. 6.9 of the EC3-1.3 [28]. Hence, α and l_a were chosen as 0.057 and 10 mm, respectively, in the calculation of nominal strength P_{EC} predicted by EC3-1.3 [28] in this study. It should be noted that the EC3-1.3 [28] does not consider the web slenderness ratio and uses the same bearing length of 10 mm for the design. Even though the LDSS specimen sections had different web slenderness ratios and were loaded by steel bearing plates with different bearing lengths in the range of 30 to 150 mm in this study.

The NAS Specification [29] provides design rules for section under web crippling in Section G5 of the specification. The design rules are suitable for sections with single web having stiffened or partially stiffened flanges. The unified equation is illustrated in Equation (8) as follows:

$$P_{NAS} = Ct^2 f_y \sin\theta \left(1 - C_R\sqrt{\frac{r_i}{t}}\right)\left(1 + C_N\sqrt{\frac{N}{t}}\right)\left(1 - C_h\sqrt{\frac{h}{t}}\right) \quad (8)$$

in which P_{NAS} = the nominal web crippling strength per web predicted by NAS [29], C = overall web crippling coefficient; C_R = inside corner radius coefficient; C_N = bearing length coefficient; C_h = web slenderness coefficient. The coefficients in the unified Equation (8) for different loading conditions with the application limits are shown in Table 6. Generally, the test specimens in this study could meet the limits, except for specimens ETF20×50×1.5N50 and ETF50×150×3.0N150 having the values of *N/h* ratio of 3.32 and 2.44, respectively, that beyond the limit of $N/h \leq 2.0$. Note that the NAS [29] does not provide design rules for loading condition of EL. Hence, the calculation of web crippling strength under loading condition of EL also used the design rules for loading conditions of EOF and ETF in this study. However, it should be noted that the ratio of *N/h* for the specimens EL20×50×1.5N30, EL20×50×1.5N50, EL60×120×3.0N120 and EL80×150×3.0N150 exceeds the limit of 2.0.

Zhou and Young [30] proposed new coefficients for the unified equation specified in the NAS [29] for web crippling of cold-formed austenitic and duplex stainless steel tubular structural members. The design equation is suitable for web crippling of cold-formed austenitic and duplex stainless steel tubular sections under the loading conditions of ETF, ITF, EOF, IOF, EL and IL. However, cold-formed LDSS sections are not covered by Zhou and Young [30]. The coefficients and the application limits proposed by Zhou and Young [30] for the unified Equation (8) are also shown in Table 6. Note that the specimens ETF20×50×1.5N50 and ETF50×150×3.0N150 exceed the limit of $N/h > 2.0$; and specimens EL20×50×1.5N30, EL20×50×1.5N50, EL40×60×2.0N60, EL60×120×3.0N120 and EL80×150×3.0N150 also exceeds the limit of $N/h > 1.6$.

4. Comparison of tests strengths with predicted strengths

The test strengths (P_{test}) of cold-formed LDSS sections per web that under the three different concentrated end bearing loads (EOF, ETF and EL) were compared with the predicted web crippling strengths calculated using the stainless steel specifications [25-27], the cold-formed carbon steel specification [29], and Zhou and Young [30]. It should be noted that the design rules in EC3-1.4 [27] refers to those specified in EC3-1.3 [28], while the design rules in the ASCE [25] and AS/NZS [26] are identical. Furthermore, it should be noted that the specimens failed near the mid-span were not included in the comparison, as they were not failed by web crippling at the specimen ends. These are the specimens EOF50×20×1.5N30, EOF60×120×3.0N90 and EOF100×100×3.0N90.

The comparison of test strengths (P_{test}) with the predicted web crippling strengths for the loading conditions of EOF, ETF and EL are shown in Tables 7-9, respectively. The ASCE [25], EC3-1.4 [27], NAS [29] specifications and Zhou and Young [30] predictions were obtained. The predicted strengths were calculated using the measured cross-section dimensions as shown in Tables 1-3. In addition, the tested material properties were used in the calculation, including the Young's moduli (E^T and E^C) and the corresponding static 0.2% proof stresses ($f_{0.2}^T$ and $f_{0.2}^C$) that obtained from the longitudinal tensile and transverse compressive coupons, as shown in Tables 4 and 5. The nominal strengths P^T and P^C were calculated using the material properties obtained from the longitudinal tensile and transverse compressive coupons, respectively.

Using the material properties of E^T and the corresponding static 0.2% proof stress of $f_{0.2}^T$ for the nominal web crippling strength predictions (P^T), for the loading condition of EOF, the mean values of tested-to-predicted strength ratio of P_{test}/P_{ASCE}^T, P_{test}/P_{EC}^T, P_{test}/P_{NAS}^T and $P_{test}/P_{Z\&Y}^T$ are 1.29, 3.02, 1.02 and 1.07, with the corresponding COVs of 0.130, 0.179, 0.090 and 0.142, for ASCE [25], EC3-1.4 [27], NAS [29] specifications and Zhou and Young [30] predictions, respectively. For the loading condition of ETF, the mean values of P_{test}/P_{ASCE}^T, P_{test}/P_{EC}^T, P_{test}/P_{NAS}^T and $P_{test}/P_{Z\&Y}^T$ are 1.81, 3.10, 0.89 and 1.36, with the corresponding COVs of 0.441, 0.445, 0.338 and 0.271, respectively. For the loading condition of EL, the mean values of P_{test}/P_{ASCE}^T, P_{test}/P_{EC}^T, P_{test}/P_{NAS}^T and $P_{test}/P_{Z\&Y}^T$ are 1.49 (2.05), 3.53, 1.07 (1.03) and 1.13, with the corresponding COVs of 0.359 (0.353), 0.357, 0.255 (0.251) and 0.271, respectively. Note that the predicted web crippling strengths for EL loading condition used the design rules of EOF (ETF) loading conditions for both ASCE [25] and NAS [29] predictions in this study, as shown in Table 9.

Overall, it is found that the predicted web crippling strengths using the design rules [25-29] are conservative for the three different loading conditions, except for the strengths predicted by the NAS Specification [29] under the loading condition of ETF. The strengths predicted by the European code [27] are much more conservative than those predicted by the ASCE specification [25], as shown in Tables 7-9. This is because European codes [27-28] do not take into consideration of the web slenderness ratio although the LDSS test specimen sections had different web slenderness in this study. Furthermore, the bearing length of 10 mm was used in the calculation for the three different loading conditions of EOF, ETF and EL, although the specimen sections were loaded by different bearing lengths from 30 to 150 mm. However, it should be noted that the web crippling design equations in ASCE [25], AS/NZS [26], NAS [29] and Zhou and Young [30] consider the web slenderness ratio *h/t* and use the actual bearing length *N* in the calculation. The web crippling strengths predicted by the NAS [29] and Zhou and Young [30] are less conservative compared with those predicted by the ASCE [25] and EC3-1.4 [27], and generally smaller values of COV, as shown in Tables 7-9. It means that the web crippling design rules specified in NAS [29] for cold-formed carbon steel and those proposed by Zhou and Young [30] for cold-formed duplex stainless steel give better predictions than those specified in the ASCE [25] and EC3-1.4 [27].

The nominal strengths (P^C) predicted using material properties of E^C and the corresponding static 0.2% proof stress of $f_{0.2}^C$ were also compared, as shown in Tables 7-9. Generally, the predictions are less conservative compared with those predicted using the material properties

of longitudinal tensile coupon tests for the cold-formed LDSS under concentrated end bearing loads, i.e., EOF, ETF and EL loading conditions. This is because the 0.2% proof stress (yield strength) obtained from the transverse compressive coupon tests are generally higher than those obtained from the longitudinal tensile coupon tests due to the cold-forming process of the sections, where the transverse direction of the tubes undergoes more cold work than the longitudinal direction as a result of the transverse bending. However, it should be noted that the predicted strengths from the ASCE [25] using material properties of tensile and compressive coupon tests are identical as the coefficients C_3 related to material properties, shown in Equation (3), was a constant value of 1.34 due to both the static 0.2% proof stresses ($f_{0.2}^{T}$ and $f_{0.2}^{C}$) are larger than 459 MPa in this study.

The comparisons of tested-to-predicted strengths using material properties from the longitudinal tensile coupon tests and transverse compression coupon tests are shown in Fig. 6(a)-(d) for ASCE [25], EC3-1.4 [27], NAS [29] and Zhou and Young [30], respectively. The three different loading conditions (EOF, ETF and EL) in which the cold-formed LDSS sections tested were included in each figure. The vertical axis plots the test strengths per web while the horizontal axis represents the predicted strengths per web. In Fig. 6(a)-(d), the results calculated using the material properties in tensile and compression were identified by "(T)" and "(C)" in the top right hand side of each label legend, respectively. Note that the predicted strengths for loading condition of EL adopted the design rules of EOF and ETF loading conditions for both the ASCE [25] and NAS [29] in this study, and they are also shown in Fig. 6(a) and (c).

5. Reliability analysis

Reliability analysis was performed for the web crippling design rules used in this study. The analysis was conducted in accordance with those specified in the Commentary of the ASCE Specification for cold-formed stainless steel members [25]. The aforementioned web crippling design provisions in the ASCE [25], EC3-1.4 [27] (EC3-1.3 [28]) for stainless steel structures, as well as those specified in NAS [29] for cold-formed carbon steel and Zhou and Young [30] for cold-formed duplex stainless steel were examined. It should be noted that the reliability analysis for the design provisions in the EC3-1.4 [27] should follow the Eurocode 0 [33]. For direct comparison, the reliability analysis that specified in the ASCE [25] was used in this study.

In this study, the reliability index (β) greater than or equal to 2.5 was set for the design provisions being considered reliable and probabilistically safe. The resistance factors (ϕ) for web crippling strength design as recommended by the ASCE [25], EC3-1.4 [27], NAS [29] and Zhou and Young [30] are shown in Tables 7-9. They were used in the calculation of the reliability index (β). In addition, the load combination of 1.2DL + 1.6LL was used for the design provisions of ASCE [25], NAS [29] and Zhou and Young [30], while the combination of 1.35DL + 1.5LL was used for European code [28], where DL represents the dead load while LL represents the live load. The ratio of 0.2 was used for DL/LL. The statistical parameters suggested in Section 6.2 of ASCE [25] were used, where M_m = 1.10, F_m = 1.00, V_M = 0.10 and V_F = 0.05, which are the mean values and coefficients of variation of material factor and fabrication factor, respectively. In addition, the mean value (P_m) and the coefficients of variation (V_P) of tests to the design prediction ratios are shown in Tables 7-9. A correction factor (C_P) in ASCE [25] was used to take consideration of the influence of limited test results. The reliability index (β) for the cold-formed LDSS tubular members under concentrated end bearing loads were calculated, and reported in Table 7-9, for the loading conditions of EOF, ETF and EL, respectively.

Using the material properties determined by the longitudinal tensile coupons in the nominal strengths calculations, the values of the reliability index (β) for the loading condition of EOF are 3.90, 5.12, 2.86 and 3.16 for ASCE [25], EC3-1.4 [27], NAS [29] and Zhou and Young [30], respectively. Similarly, the values of the β for the loading condition of ETF are 2.73, 3.15, 1.15 and 2.75, and the values of the β for the loading condition of EL are 2.78 (3.53), 4.03, 2.22 (1.80) and 2.28, for ASCE [25], EC3-1.4 [27], NAS [29] and Zhou and Young [30], respectively. Note that the predicted strengths for loading condition of EL used the design rules for loading condition of EOF (ETF) for ASCE [25] and NAS [29] in this study. Generally, it is found that the design provisions [25-27] are reliable and probabilistically safe for the web crippling design of cold-formed LDSS tubular sections under the three different concentrated end bearing loads as the values of reliability index (β) are greater than the target value of 2.5. However, the values of β are smaller than the target value of 2.5 for the ETF loading condition in the NAS [29], as well as for the EL loading condition in the NAS [29] and Zhou and Young [30]. In addition, using the material properties determined by the transverse compressive coupons in the nominal strength calculations, it is found that the design rules [25-27, 29-30] are reliable and probabilistically safe for the web crippling design of LDSS sections under concentrated end bearing loads, except the provisions in the NAS [29] for ETF and EL loading conditions.

6. Conclusions

A series of tests was conducted to investigate the web crippling behaviour of cold-formed lean duplex stainless steel (LDSS) tubular sections under concentrated end bearing loads. The test specimens had the web slenderness ratio ranged from 9.8 to 43.5, and loaded with different bearing lengths. The tubular sections were tested under three different concentrated end bearing loads, namely, the loading conditions of End-One-Flange (EOF), End-Two-Flange (ETF) and end loading (EL). The strengths obtained from the tests were compared with the predicted strengths calculated using the ASCE [25], AS/NZS [26] and EC3-1.4 [27] stainless steel specifications. In addition, the web crippling strength predicted by the NAS Specification [29] for cold-formed carbon steel structures and Zhou and Young [30] for cold-formed duplex stainless steel tubular sections were also compared with the test strengths. In the calculation of the predicted strengths, both the material properties determined by longitudinal tensile coupons and compressive coupons were used. The reliability of the aforementioned design rules was assessed.

It is found that the predicted strengths calculated using the ASCE [25], AS/NZS [26] and EC3-1.4 [27] for stainless steel structures are quite conservative but reliable for the cold-formed LDSS under the three different concentrated end bearing loads, where the predictions from the EC3-1.4 [27] are much more conservative. The existing codified web crippling design provisions for stainless steel structures are not able to predict the nominal strengths of cold-formed LDSS tubular sections under concentrated end bearing loads accurately. The predictions calculated using the design provisions in the NAS [29] and Zhou and Young [30] are generally conservative, but less conservative compared with the predictions by ASCE [25], AS/NZS [26] and EC3-1.4 [27]. However, the predictions by the NAS [29] are unconservative and not reliable for the loading condition of ETF. By using the material properties determined by the longitudinal tensile coupons, both predictions by the NAS [29] and Zhou and Young [30] are not reliable for the loading condition of EL.

Acknowledgements

The authors are grateful to STALA Tube Finland for providing the test specimens. The research work described in this paper was supported by a grant from the Research Grants Council of the Hong Kong Special Administrative Region, China (Project No. HKU17209614E). The authors are also grateful to Miss Ning Yan CHAN for her assistance in the experimental program as part of her final year undergraduate research project at the University of Hong Kong.

References

[1] Saliba, N. and Gardner, L. Cross-section stability of lean duplex stainless steel welded I-sections. Journal of Constructional Steel Research 2013, 18: 1-14.

[2] Huang, Y. and Young, B. Material properties of cold-formed lean duplex stainless steel sections. Thin-Walled Structures 2012, 54: 72 - 81.

[3] Huang, Y. and Young, B. Experimental and numerical investigation of cold-formed lean duplex stainless steel flexural members. Thin-Walled Structures 2014, 73: 216 - 228.

[4] Theofanous, M. and Gardner L. Experimental and numerical studies of lean duplex stainless steel beams. Journal of Constructional Steel Research 2010, 66: 816-825.

[5] Theofanous, M. and Gardner L. Testing and numerical modelling of lean duplex stainless steel hollow section columns. Engineering Structures 2009, 31: 3047-3058.

[6] Huang, Y. and Young, B. Tests of pin-ended cold-formed lean duplex stainless steel columns. Journal of Constructional Steel Research 2013, 82: 203 - 215.

[7] Huang, Y. and Young, B. Structural performance of cold-formed lean duplex stainless steel columns. Thin-Walled Structures 2014, 83: 59 – 69.

[8] Huang, Y. and Young, B. Experimental investigation of cold-formed lean duplex stainless steel beam-columns. Thin-Walled Structures 2014, 76: 105 - 117.

[9] Huang, Y. and Young, B. Design of cold-formed lean duplex stainless steel members in combined compression and bending. Journal of Structural Engineering ASCE 2014, 141 (5): 04014138.

[10] Saliba, N. and Gardner L. Experimental study of the shear response of lean duplex stainless steel plate girders. Engineering Structures 2013, 46: 375-391.

[11] Saliba N., Real, E., Gardner, L. Shear design recommendations for stainless steel plate girders. Engineering Structures 2014, 59: 220-228.

[12] Cai, Y. and Young, B. Structural behavior of cold-formed stainless steel bolted connections. Thin-Walled Structures 2014, 83: 147-156.

[13] Cai, Y. and Young, B. Behavior of cold-formed stainless steel single shear bolted connections at elevated temperatures. Thin-Walled Structures 2014, 75: 63-75.

[14] Cai, Y. and Young, B. Transient state tests of cold-formed stainless steel single shear bolted connections. Engineering Structures 2014, 81: 1-9.

[15] Cai, Y. and Young, B. High temperature tests of cold-formed stainless steel double shear bolted connections. Journal of Constructional Steel Research 2015, 104: 49-63.

[16] Korvink, S.A. and van den Berg, G.J. Web crippling of stainless steel cold-formed beams. Proceedings of the Twelfth International Specialty Conference on Cold-Formed Steel Structures, University of Missouri-Rolla, St. Louis, Missouri, USA, 1994.

[17] Korvink, S.A., van den Berg, G.J. and van der Merwe, P. Web crippling of stainless steel cold-formed beams. Journal of Construction Steel Research 1995, 34: 225–248.
[18] Talja, A. and Salmi, P. Design of stainless steel RHS beams, columns and beam-columns. Research note 1619, VTT Building Technology, Finland, 1995.
[19] Gardner, L., Talja, A. and Baddoo, N.R. Structural design of high-strength austenitic stainless steel. Thin-Walled Structures 2006, 44: 517–528.
[20] Zhou, F. and Young, B. Cold-formed stainless steel sections subjected to web crippling. Journal of Structural Engineering 2006, 132(1): 134–144.
[21] Zhou, F. and Young, B. Cold-formed high-strength stainless steel tubular sections subjected to web crippling. Journal of Structural Engineering 2007, 133(3): 368–377.
[22] Zhou, F. and Young, B. Experimental and numerical investigations of cold-formed stainless steel tubular sections subjected to concentrated bearing load. Journal of Constructional Steel Research 2007, 63(11): 1452–1466.
[23] Bock, M., Arrayago, I., Real, E. and Mirambell, E. Study of web crippling in ferritic stainless steel cold formed sections. Thin-Walled Structures 2013, 69: 29–44.
[24] Li, H-T. and Young, B. Cold-formed ferritic stainless steel tubular structural members subjected to concentrated bearing loads. Engineering Structures 2017, 145: 392-405.
[25] ASCE. Specification for the design of cold-formed stainless steel structural members. American Society of Civil Engineers (ASCE), ASCE Standard, SEI/ASCE-8-02, Reston, Virginia, 2002.
[26] AS/NZS. Cold-formed stainless steel structures. AS/NZS 4673:2001, Australian/New Zealand Standard (AS/NZS), Standards Australia, Sydney, Australia, 2001.
[27] EC3-1.4. Eurocode 3. Design of steel structures - Part 1.4: General rules - Supplementary rules for stainless steels. EN 1993-1-4:2006+A1:2015, Brussels, Belgium, European Committee for Standardization, 2015.
[28] EC3-1.3. Eurocode 3: Design of steel structures - Part 1–3: General rules – Supplementary rules for cold-formed members and sheeting. EN 1993-1-3, Brussels, Belgium: European committee for standardization; 2006.
[29] North American Specification (NAS). North American Specification for the design of cold-formed steel structural members. AISI S100–16, Washington D. C., USA: American Iron and Steel Institute (AISI); 2016.
[30] Zhou, F. and Young, B. Web crippling of cold-formed steel tubular sections. Advances in Structural engineering, 2008, Vol. 11, No. 6, 679-691.
[31] American Society for Testing and Materials (ASTM). Standard test methods for tension testing of metallic materials. E8/E8M-15a, West Conshohocken, PA., USA: ASTM International; 2016.

[32] Huang, Y. and Young, B. The art of coupon tests. Journal of Constructional Steel Research 2014, 96: 159-175.

[33] EC0. Eurocode 0: basis of structural design. EN 1990:2002+A1:2005. Brussels, Belgium: European committee for standardization; 2005.

Nomenclature

B overall width of cross section

E^T Young's modulus obtained from longitudinal tensile coupon test

E^C Young's modulus obtained from transverse compressive coupon test

H overall depth of cross section

L length of test specimen

N bearing length

P^C nominal web crippling strength per web calculated using material properties in compressive coupon test

P^T nominal web crippling strength per web calculated using material properties in longitudinal tensile coupon test

P_{ASCE} nominal web crippling strength per web obtained from ASCE Specification

P_{ASCE}^T nominal web crippling strength per web obtained from ASCE Specification using longitudinal tensile coupon tests

P_{ASCE}^C nominal web crippling strength per web obtained from ASCE Specification using transverse compressive coupon tests

P_{EC} nominal web crippling strength per web obtained from European Code

P_{EC}^T nominal web crippling strength per web obtained from European Code using longitudinal tensile coupon tests

P_{EC}^C nominal web crippling strength per web obtained from European Code using transverse compressive coupon tests

P_{NAS} nominal web crippling strength per web obtained from North American Specification

P_{NAS}^T nominal web crippling strength per web obtained from North American Specification using longitudinal tensile coupon tests

P_{NAS}^C nominal web crippling strength per web obtained from North American Specification using transverse compressive coupon tests

P_{test} experimental web crippling strength per web

$P_{Z\&Y}$ nominal web crippling strength per web obtained from Zhou & Young's proposal

$P_{Z\&Y}^T$ nominal web crippling strength per web obtained from Zhou & Young's proposal using longitudinal tensile coupon tests

$P_{Z\&Y}^C$ nominal web crippling strength per web obtained from Zhou & Young's proposal using transverse compressive coupon tests

P_m mean value of tested-to-predicted load ratio

r_i inner corner radius

V_P coefficient of variation of tested-to-predicted load ratio

h depth of flat portion of web

n^c Ramerg-Osgood parameter obtained from transverse compressive coupon test

n^T Ramberg-Osgood parameter obtained from longitudinal tensile coupon test

t web thickness

β reliability index

ε_f^T	strain after fracture from longitudinal tensile coupon test
ε_u^T	strain at ultimate tensile strength from longitudinal tensile coupon test
ϕ	resistance factor
$f_{0.01}^T$	static 0.01% proof stress obtained from longitudinal tensile coupon test
$f_{0.2}^T$	static 0.2% proof stress obtained from longitudinal tensile coupon test
f_u^T	static tensile strength obtained from longitudinal tensile coupon test
$f_{0.01}^C$	static 0.01% proof stress obtained from transverse compressive test
$f_{0.2}^C$	static 0.2% proof stress obtained from transverse compressive coupon test

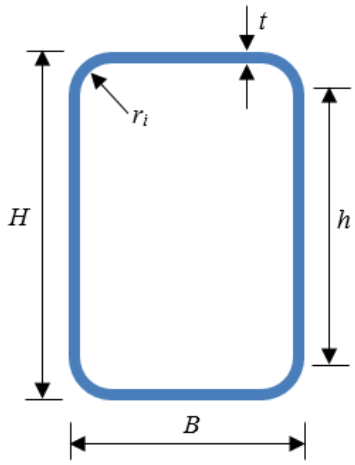

Figure 1: Definition of symbols

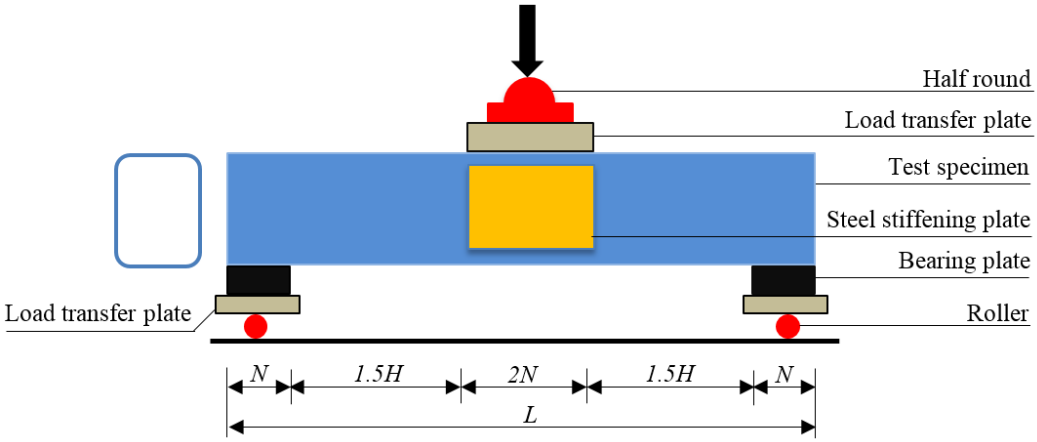

(a) End-One-Flange (EOF) loading condition

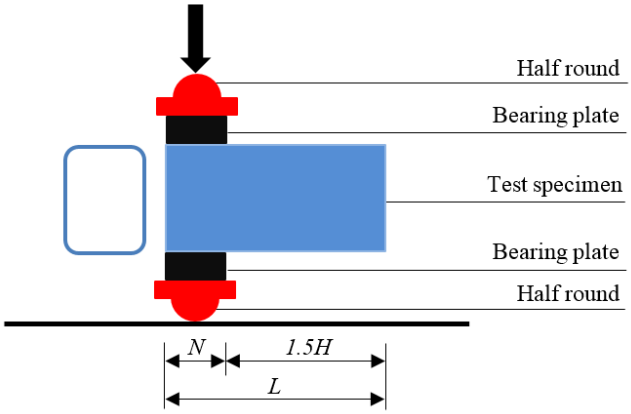

(b) End-Two-Flange (ETF) loading condition

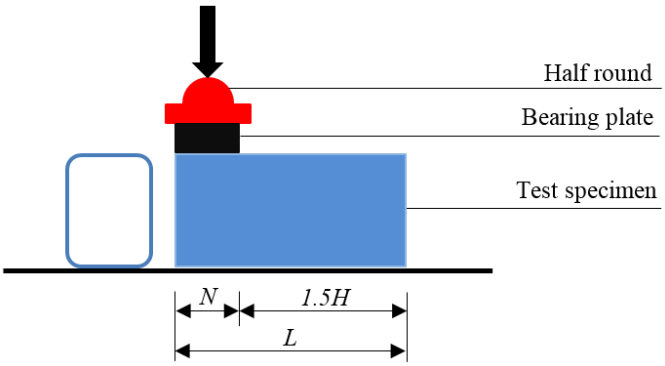

(c) End loading (EL) condition

Figure 2: Sections under different concentrated end bearing loads

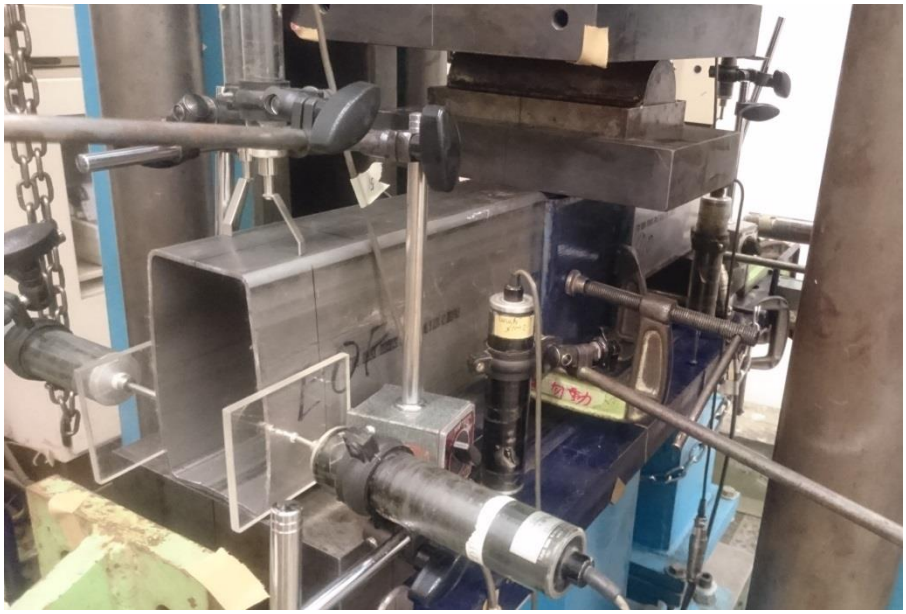

(a) Specimen EOF150×80×3.0N90

(b) Specimen ETF80×150×3.0N150

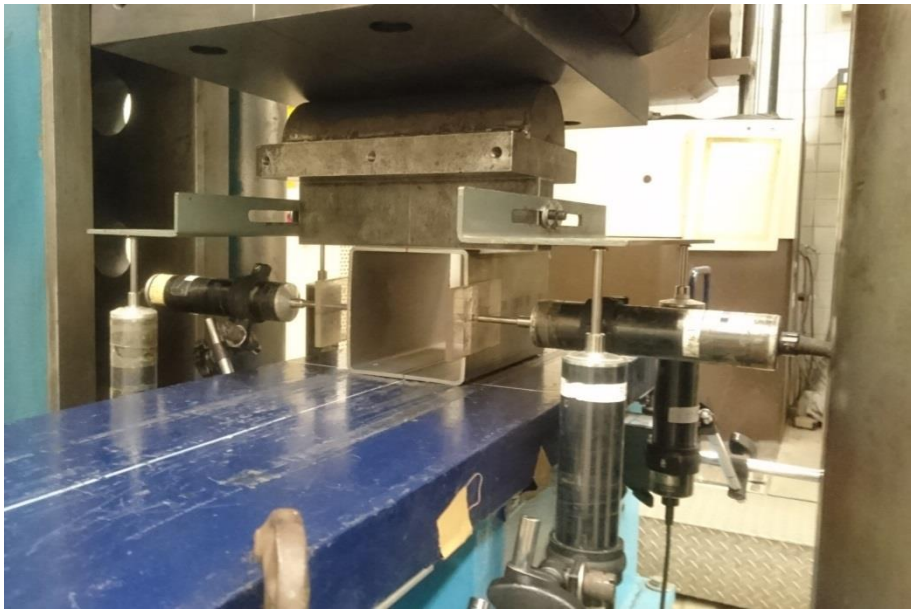

(c) Specimen EL100×100×3.0N30

Figure 3: Test setup of specimens under concentrated end bearing loads

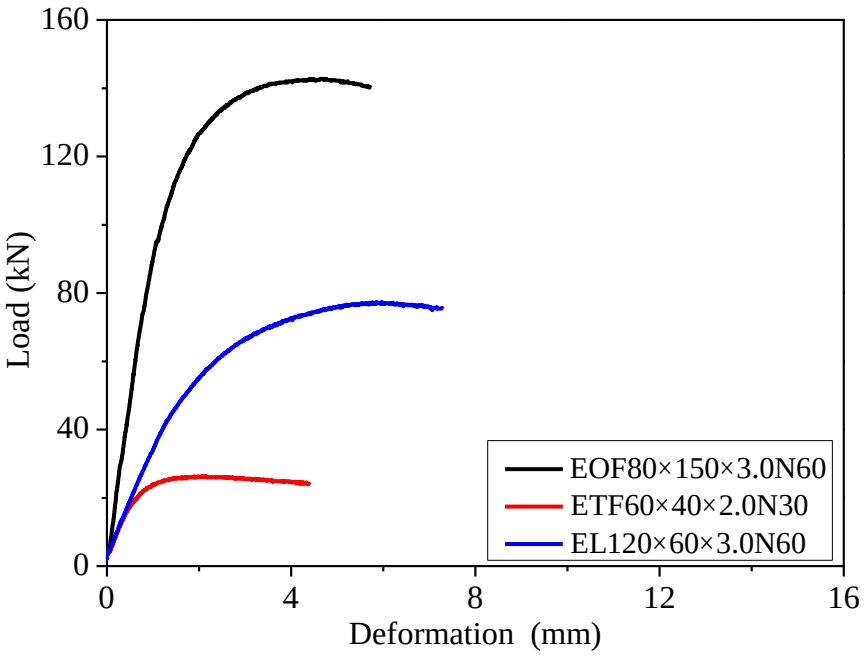

(a) Load-vertical deformation

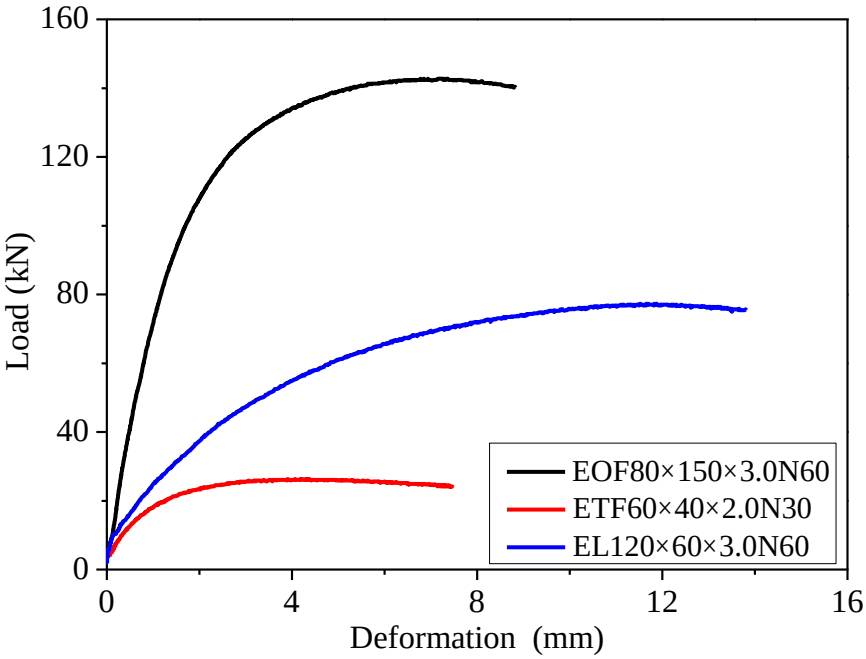

(b) Load-lateral deformation

Figure 4: Load-deformation curves of specimens under concentrated end bearing loads

(a) Original section of 150×80×3.0

(b) EOF150×80×3.0N90

(c) ETF150×80×3.0N90

(d) EL150×80×3.0N90

Figure 5: Web crippling failure of specimens (b-d) under concentrated end bearing loads

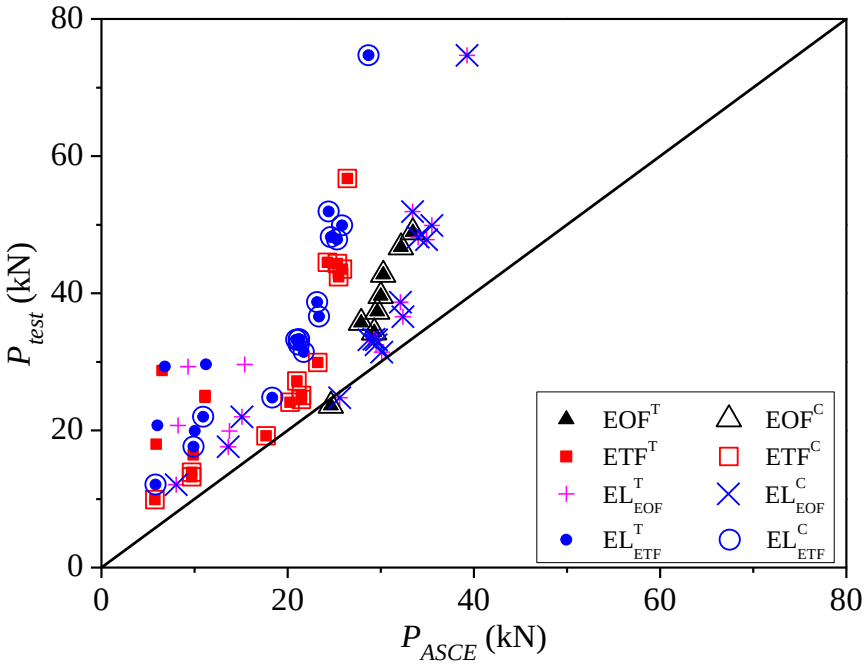

(a) Predictions by ASCE Specification [25]

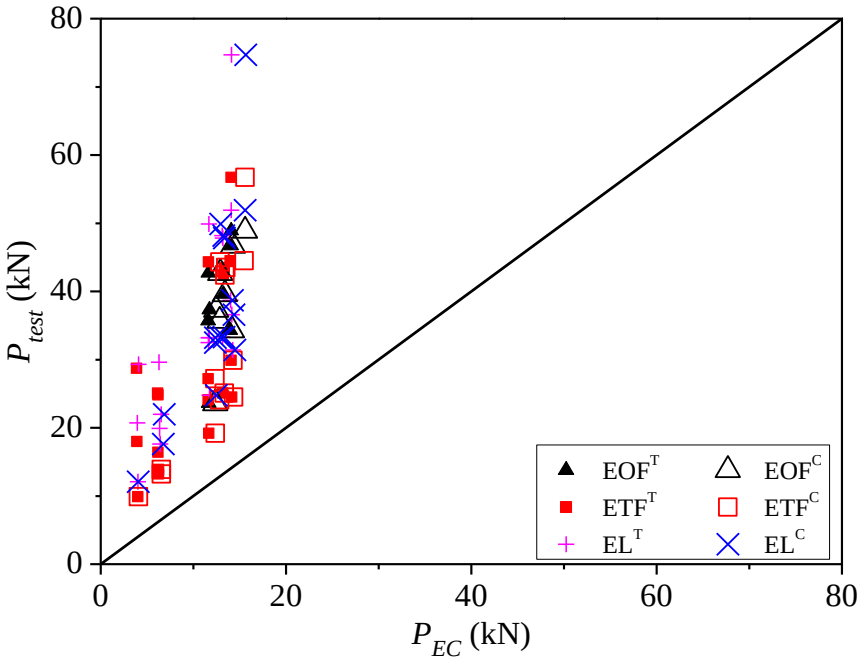

(b) Predictions by Euro Code [27]

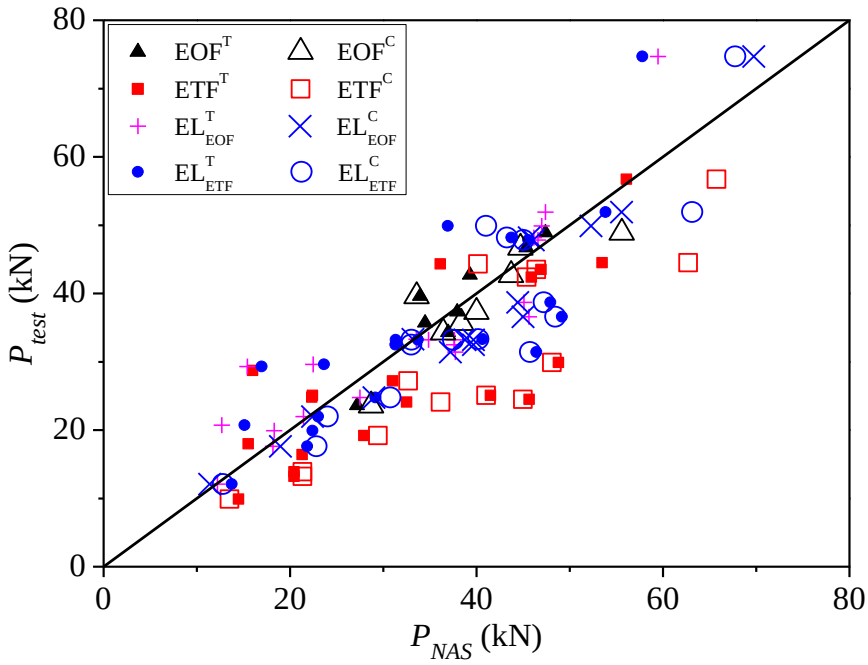

(c) Predictions by NAS Specification [29]

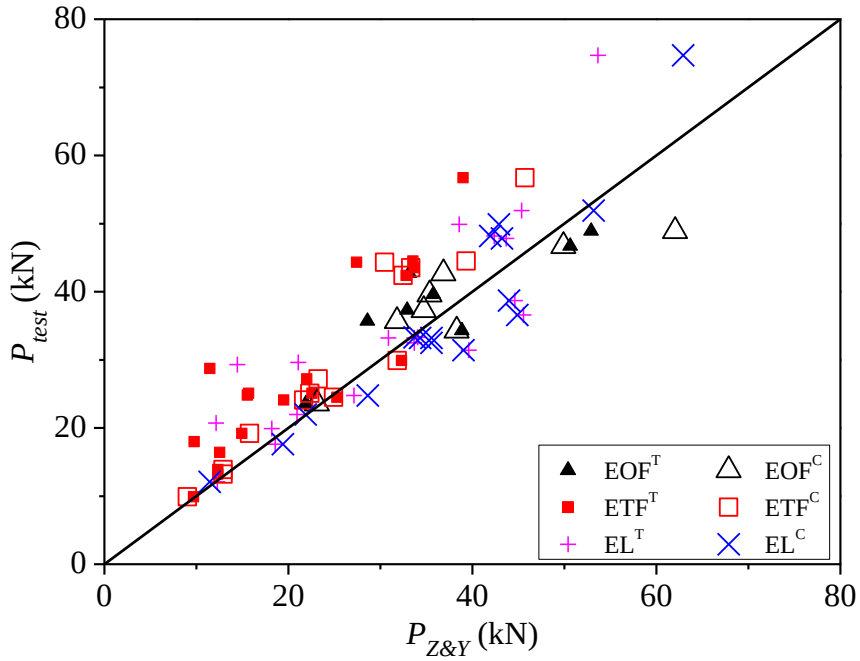

(d) Predictions by Zhou and Young [30]

Figure 6: Composion of test strengths with predicted strengths by different provisions

Table 1: Measured dimensions and test strengths for specimens under EOF loading condition

Specimen	***H*** (mm)	***B*** (mm)	***t*** (mm)	r_i (mm)	***L*** (mm)	***h/t***	r_i/t	***N/t***	***N/h***	P_{test} (kN)
EOF50×20×1.5N30	50.2	20.2	1.51	1.0	270.2	29.9	0.7	19.8	0.66	13.0*
EOF60×120×3.0N60	60.0	119.9	3.07	2.9	421.4	15.7	0.9	19.5	1.25	48.9
EOF60×120×3.0N90	60.2	120.1	3.07	3.3	542.7	15.5	1.1	29.3	1.89	46.6*
EOF80×150×3.0N60	80.2	151.9	3.08	6.5	480.2	19.8	2.1	19.5	0.98	35.7
EOF80×150×3.0N90	80.9	151.8	3.09	6.5	510.1	20.0	2.1	29.1	1.46	42.7
EOF100×100×3.0N30	100.3	100.2	3.09	3.3	420.3	28.4	1.1	9.7	0.34	39.6
EOF100×100×3.0N90	100.3	100.1	3.08	3.1	659.2	28.5	1.0	29.2	1.02	61.9*
EOF120×60×3.0N30	120.0	60.1	3.07	3.3	482.5	35.0	1.1	9.8	0.28	34.3
EOF120×60×3.0N60	119.9	60.1	3.07	2.9	599.5	35.2	0.9	19.5	0.56	46.7
EOF150×80×3.0N30	151.6	80.1	3.09	6.5	570.2	42.8	2.1	9.7	0.23	23.6
EOF150×80×3.0N90	151.5	80.1	3.10	6.2	810.0	42.9	2.0	29.1	0.68	37.3

*Note: Specimen failed near mid-span.

Table 2: Measured dimensions and test strengths for specimens under ETF loading condition

Specimen	***H*** (mm)	***B*** (mm)	***t*** (mm)	r_i (mm)	***L*** (mm)	***h/t***	r_i/t	***N/t***	***N/h***	P_{test} (kN)
ETF20×50×1.5N30	19.9	50.2	1.50	0.8	60.0	10.2	0.6	20.1	1.97	18.0
ETF20×50×1.5N50	19.9	50.1	1.49	0.9	80.5	10.1	0.6	33.5	3.32	28.7
ETF40×60×2.0N30	40.4	60.2	1.99	1.9	90.6	16.4	0.9	15.1	0.92	16.4
ETF40×60×2.0N60	40.4	60.2	2.00	2.1	121.2	16.1	1.1	30.0	1.87	24.8
ETF40×60×2.0N60-r	40.4	60.3	1.99	2.0	120.9	16.3	1.0	30.2	1.85	25.1
ETF50×20×1.5N30	50.2	19.9	1.52	0.8	105.2	30.1	0.5	19.8	0.66	9.9
ETF60×40×2.0N30	60.2	40.3	2.00	1.9	120.8	26.2	0.9	15.0	0.57	13.2
ETF60×40×2.0N30-r	60.2	40.1	2.00	1.9	120.5	26.2	0.9	15.0	0.57	13.9
ETF60×120×3.0N60	60.0	120.0	3.06	2.9	151.2	15.7	0.9	19.6	1.25	44.5
ETF60×120×3.0N90	59.9	119.9	3.07	2.9	180.8	15.6	0.9	29.3	1.88	56.7
ETF80×150×3.0N60	80.9	151.1	3.08	6.5	180.3	20.0	2.1	19.5	0.97	24.1
ETF80×150×3.0N150	80.7	150.7	3.09	6.5	269.3	19.9	2.1	48.6	2.44	44.3
ETF100×100×3.0N30	100.5	100.3	3.08	3.4	180.2	28.4	1.1	9.7	0.34	25.1
ETF100×100×3.0N90	100.4	100.1	3.09	3.4	240.3	28.3	1.1	29.2	1.03	42.4
ETF100×100×3.0N90-r	100.4	100.1	3.09	3.1	240.0	28.4	1.0	29.1	1.02	43.5
ETF120×60×3.0N30	120.4	59.8	3.09	3.3	211.1	34.9	1.1	9.7	0.28	24.5
ETF120×60×3.0N60	120.1	60.2	3.07	2.9	240.9	35.2	0.9	19.5	0.55	29.9
ETF150×80×3.0N30	151.0	80.3	3.09	6.5	255.0	42.6	2.1	9.7	0.23	19.2
ETF150×80×3.0N90	151.0	80.2	3.08	6.2	314.8	43.0	2.0	29.2	0.68	27.2

Table 3: Measured dimensions and test strengths for specimens under EL loading condition

Specimen	***H*** (mm)	***B*** (mm)	***t*** (mm)	r_i (mm)	***L*** (mm)	***h/t***	r_i/t	***N/t***	***N/h***	P_{test} (kN)
EL20×50×1.5N30	20.1	50.2	1.51	1.1	60.3	9.8	0.7	19.8	2.03	20.7
EL20×50×1.5N50	20.1	50.1	1.53	0.9	80.2	10.0	0.6	32.7	3.27	29.3
EL40×60×2.0N30	40.4	60.2	2.01	1.6	90.8	16.5	0.8	14.9	0.91	19.9
EL40×60×2.0N60	40.5	60.3	2.00	1.6	120.4	16.6	0.8	30.0	1.81	29.6
EL50×20×1.5N30	50.2	20.1	1.53	1.1	105.3	29.4	0.7	19.7	0.67	12.1
EL60×40×2.0N30	60.3	40.4	2.02	1.5	124.1	26.4	0.7	14.9	0.56	17.6
EL60×40×2.0N50	60.4	40.3	2.04	1.6	211.2	26.0	0.8	24.5	0.94	22.0
EL60×120×3.0N60	60.3	120.1	3.07	2.9	150.5	15.8	0.9	19.5	1.24	51.9
EL60×120×3.0N120	60.3	119.9	3.08	3.0	209.6	15.6	1.0	39.0	2.49	74.7
EL80×150×3.0N60	80.1	150.8	3.09	6.0	180.7	20.1	1.9	19.4	0.97	33.2
EL80×150×3.0N150	80.8	150.6	3.09	6.1	270.5	20.2	2.0	48.6	2.41	49.9
EL100×100×3.0N30	100.3	100.1	3.09	3.8	180.7	28.1	1.2	9.7	0.35	33.3
EL100×100×3.0N90	100.4	100.2	3.09	4.1	240.2	27.8	1.3	29.1	1.05	48.2
EL100×100×3.0N90-r	100.4	100.1	3.08	3.4	240.2	28.4	1.1	29.2	1.03	47.8
EL120×60×3.0N30	119.9	60.0	3.10	3.1	207.9	34.7	1.0	9.7	0.28	31.4
EL120×60×3.0N60	119.9	60.5	3.07	3.1	241.9	35.0	1.0	19.5	0.56	38.7
EL120×60×3.0N60-r	120.0	60.5	3.08	2.9	242.5	35.1	0.9	19.5	0.56	36.6
EL150×80×3.0N30	150.9	80.3	3.09	5.8	256.3	43.2	1.9	9.7	0.23	24.8
EL150×80×3.0N90	152.0	80.6	3.08	6.0	316.0	43.5	1.9	29.2	0.67	32.5
EL150×80×3.0N90-r	151.0	80.6	3.08	6.0	315.7	43.2	1.9	29.2	0.68	33.2

Table 4: Material properties of lean duplex stainless steel by tensile coupon tests

Stainless steel grade	Section $H\times B\times t$ (mm)	Material properties from static curves						
		E^T	$f_{0.01}^T$	$f_{0.2}^T$	f_u^T	ε_u^T	ε_f^T	n^T
		GPa	MPa	MPa	MPa	%	%	
EN 1.4162	50×20×1.5	194	384	656	777	33.2	42.2	5.6
EN 1.4062	60×40×2.0	199	340	600	756	25.9	40.3	5.3
	100×100×3.0	202	365	557	701	26.4	43.1	7.1
	120×60×3.0	206	423	620	736	25.5	38.5	7.8
	150×80×3.0	194	263	491	722	29.6	43.3	4.8

Table 5: Material properties of lean duplex stainless steel by compressive coupon tests

Stainless steel grade	Section $H\times B\times t$ (mm)	Material properties from static curves			
		E^C	$f_{0.01}^C$	$f_{0.2}^C$	n^C
		GPa	MPa	MPa	
EN 1.4162	50×20×1.5	212	346	611	5.3
EN 1.4062	60×40×2.0	211	378	627	5.9
	60×120×3.0	215	421	727	5.5
	80×150×3.0	214	315	546	5.4
	100×100×3.0	209	353	551	6.7
	120×60×3.0	215	382	611	6.4
	150×80×3.0	208	268	518	4.5

Table 6: Coefficients for web crippling design of cold-formed steel sections

Provision	Steel	Section type	Load condition	Coefficients					Limits			
				C	C_R	C_N	C_h	ϕ	r_i/t	N/t	h/t	N/h
NAS [29]	Carbon steel	single web channel	EOF	4.0	0.14	0.35	0.02	0.80	≤ 5	≤ 210	≤ 200	≤ 2.0
			ETF	13.0	0.32	0.05	0.04	0.90	≤ 3	≤ 210	≤ 200	≤ 2.0
Zhou and Young [30]	Duplex stainless steel	Square and rectangular hollow sections	EOF	5.0	0.40	0.50	0.020	0.70	≤ 2	≤ 50	≤ 50	≤ 2.0
			ETF	3.0	0.36	0.50	0.020	0.80	≤ 2	≤ 50	≤ 50	≤ 2.0
			EL	5.8	0.26	0.18	0.001	0.80	≤ 2	≤ 50	≤ 200	≤ 1.6

Note: The table is suitable to stiffened or partially stiffened flanges that unfastened to support.

Table 7: Comparison of test strengths with predicted strengths for EOF loading condition

Specimen	P_{test} (kN)	***Using material properties from tensile coupons***				***Using material properties from compressive coupons***			
		P_{test}/P^{T}_{ASCE}	P_{test}/P^{T}_{EC}	P_{test}/P^{T}_{NAS}	$P_{test}/P^{T}_{Z\&Y}$	P_{test}/P^{C}_{ASCE}	P_{test}/P^{C}_{EC}	P_{test}/P^{C}_{NAS}	$P_{test}/P^{C}_{Z\&Y}$
EOF50×20×1.5N30	13.0*	-	-	-	-	-	-	-	-
EOF60×120×3.0N60	48.9	1.46	3.48	1.03	0.92	1.46	3.14	0.88	0.79
EOF60×120×3.0N90	46.6*	-	-	-	-	-	-	-	-
EOF80×150×3.0N60	35.7	1.28	3.08	1.04	1.25	1.28	2.78	0.93	1.12
EOF80×150×3.0N90	42.7	1.41	3.67	1.09	1.29	1.41	3.31	0.98	1.16
EOF100×100×3.0N30	39.6	1.32	2.99	1.17	1.11	1.32	2.95	1.18	1.12
EOF100×100×3.0N90	61.9*	-	-	-	-	-	-	-	-
EOF120×60×3.0N30	34.3	1.17	2.45	0.93	0.88	1.17	2.42	0.94	0.90
EOF120×60×3.0N60	46.7	1.45	3.32	1.03	0.92	1.45	3.27	1.04	0.94
EOF150×80×3.0N30	23.6	0.96	2.02	0.87	1.08	0.96	1.90	0.82	1.02
EOF150×80×3.0N90	37.3	1.26	3.17	0.98	1.13	1.26	2.99	0.93	1.07
Mean, P_m		1.29	3.02	1.02	1.07	1.29	2.84	0.96	1.01
COV, V_p		0.130	0.179	0.090	0.142	0.130	0.167	0.113	0.128
Resistance factor, ϕ		0.70	0.91	0.80	0.70	0.70	0.91	0.80	0.70
Reliability index, β		3.90	5.12	2.86	3.16	3.90	5.09	2.53	3.08

*Note: Specimen failed near mid-span, not included in the comparison.

Table 8: Comparison of test strengths with predicted strengths for ETF loading condition

Specimen	P_{test} (kN)	***Using material properties from tensile coupons***				***Using material properties from compressive coupons***			
		P_{test}/P^{T}_{ASCE}	P_{test}/P^{T}_{EC}	P_{test}/P^{T}_{NAS}	$P_{test}/P^{T}_{Z\&Y}$	P_{test}/P^{C}_{ASCE}	P_{test}/P^{C}_{EC}	P_{test}/P^{C}_{NAS}	$P_{test}/P^{C}_{Z\&Y}$
ETF20×50×1.5N30	18.0	3.05	4.59	1.16	1.84	-	-	-	-
ETF20×50×1.5N50	28.7	4.40	7.39	1.79	2.50	-	-	-	-
ETF40×60×2.0N30	16.4	1.66	2.65	0.77	1.31	-	-	-	-
ETF40×60×2.0N60	24.8	2.22	4.00	1.11	1.59	-	-	-	-
ETF40×60×2.0N60-r	25.1	2.25	4.07	1.12	1.60	-	-	-	-
ETF50×20×1.5N30	9.9	1.72	2.46	0.68	1.02	1.72	2.43	0.73	1.10
ETF60×40×2.0N30	13.2	1.36	2.12	0.65	1.07	1.36	2.01	0.62	1.02
ETF60×40×2.0N30-r	13.9	1.43	2.23	0.68	1.13	1.43	2.11	0.65	1.08
ETF60×120×3.0N60	44.5	1.83	3.18	0.83	1.33	1.83	2.87	0.71	1.13
ETF60×120×3.0N90	56.7	2.15	4.03	1.01	1.45	2.15	3.64	0.86	1.24
ETF80×150×3.0N60	24.1	1.19	2.08	0.74	1.24	1.19	1.88	0.67	1.11
ETF80×150×3.0N150	44.3	1.75	3.81	1.23	1.62	1.75	3.44	1.10	1.45
ETF100×100×3.0N30	25.1	1.17	1.91	0.60	1.11	1.17	1.88	0.61	1.12
ETF100×100×3.0N90	42.4	1.66	3.20	0.92	1.29	1.66	3.16	0.93	1.31
ETF100×100×3.0N90-r	43.5	1.68	3.26	0.93	1.29	1.68	3.22	0.94	1.31
ETF120×60×3.0N30	24.5	1.14	1.73	0.54	0.97	1.14	1.71	0.54	0.98
ETF120×60×3.0N60	29.9	1.29	2.13	0.61	0.93	1.29	2.09	0.62	0.94
ETF150×80×3.0N30	19.2	1.09	1.65	0.69	1.28	1.09	1.55	0.65	1.22
ETF150×80×3.0N90	27.2	1.29	2.34	0.88	1.24	1.29	2.21	0.83	1.17
Mean, P_m		1.81	3.10	0.89	1.36	1.48	2.44	0.75	1.16
COV, V_p		0.441	0.445	0.338	0.271	0.215	0.282	0.215	0.121
Resistance factor, ϕ		0.70	0.91	0.90	0.80	0.70	0.91	0.90	0.80
Reliability index, β		2.73	3.15	1.15	2.75	3.73	3.69	0.97	3.22

Table 9: Comparison of test strengths with predicted strengths for EL loading condition

Specimen	P_{test} (kN)	*Using material properties from tensile coupons*						*Using material properties from compressive coupons*					
		P_{test}/P^{T}_{ASCE}		P_{test}/P^{T}_{EC}	P_{test}/P^{T}_{NAS}		$P_{test}/P^{T}_{Z\&Y}$	P_{test}/P^{C}_{ASCE}		P_{test}/P^{C}_{EC}	P_{test}/P^{C}_{NAS}		$P_{test}/P^{C}_{Z\&Y}$
	EL	EOF	ETF	EL	EOF	ETF	EL	EOF	ETF	EL	EOF	ETF	EL
EL20×50×1.5N30	20.7	2.52	3.43	5.24	1.63	1.37	1.71	-	-	-	-	-	-
EL20×50×1.5N50	29.3	3.15	4.30	7.20	1.90	1.73	2.03	-	-	-	-	-	-
EL40×60×2.0N30	19.9	1.45	1.98	3.14	1.09	0.89	1.09	-	-	-	-	-	-
EL40×60×2.0N60	29.6	1.92	2.63	4.71	1.32	1.25	1.40	-	-	-	-	-	-
EL50×20×2.0N30	12.1	1.50	2.08	3.02	0.99	0.88	0.98	1.50	2.08	2.99	1.06	0.95	1.06
EL60×40×2.0N30	17.6	1.29	1.78	2.74	0.97	0.81	0.95	1.29	1.78	2.60	0.93	0.77	0.91
EL60×40×2.0N50	22.0	1.46	2.01	3.37	1.03	0.96	1.05	1.46	2.01	3.20	0.98	0.91	1.01
EL60×120×3.0N60	51.9	1.55	2.13	3.69	1.10	0.96	1.14	1.55	2.13	3.33	0.93	0.82	0.98
EL60×120×3.0N120	74.7	1.90	2.60	5.29	1.26	1.29	1.39	1.90	2.60	4.78	1.07	1.10	1.19
EL80×150×3.0N60	33.2	1.16	1.59	2.84	0.95	0.98	1.08	1.16	1.59	2.56	0.86	0.89	0.97
EL80×150×3.0N150	49.9	1.41	1.93	4.27	1.06	1.35	1.29	1.41	1.93	3.86	0.95	1.22	1.16
EL100×100×3.0N30	33.3	1.14	1.57	2.54	0.99	0.82	0.98	1.14	1.57	2.50	1.00	0.83	0.99
EL100×100×3.0N90	48.2	1.42	1.95	3.67	1.04	1.10	1.14	1.42	1.95	3.63	1.06	1.11	1.15
EL100×100×3.0N90-r	47.8	1.37	1.89	3.63	1.03	1.05	1.09	1.37	1.89	3.58	1.04	1.06	1.11
EL120×60×3.0N30	31.4	1.04	1.44	2.20	0.83	0.68	0.79	1.04	1.44	2.17	0.84	0.69	0.80
EL120×60×3.0N60	38.7	1.21	1.67	2.76	0.86	0.81	0.87	1.21	1.67	2.72	0.87	0.82	0.88
EL120×60×3.0N60-r	36.6	1.13	1.57	2.59	0.80	0.74	0.80	1.13	1.57	2.55	0.81	0.76	0.82
EL150×80×3.0N30	24.8	0.97	1.35	2.11	0.90	0.85	0.91	0.97	1.35	1.99	0.85	0.80	0.86
EL150×80×3.0N90	32.5	1.10	1.53	2.79	0.86	1.04	0.96	1.10	1.53	2.63	0.82	0.98	0.91
EL150×80×3.0N90-r	33.2	1.12	1.57	2.85	0.88	1.06	0.99	1.12	1.57	2.69	0.84	1.00	0.93
Mean, P_m		1.49	2.05	3.53	1.07	1.03	1.13	1.30	1.79	2.99	0.93	0.92	0.98
COV, V_p		0.359	0.353	0.357	0.255	0.251	0.271	0.184	0.180	0.239	0.100	0.163	0.124
Resistance factor, ϕ		0.70	0.70	0.91	0.80	0.90	0.80	0.70	0.70	0.91	0.80	0.90	0.80
Reliability index, β		2.78	3.53	4.03	2.22	1.80	2.28	3.61	4.69	4.68	2.54	1.79	2.62